Formation of shallow boron emitters in crystalline silicon using flash lamp annealing: Role of excess silicon interstitials

Heine Nygard Riise,[1,a)] Thomas Schumann,[2] Alexander Azarov,[1] Renè Hübner,[2] Wolfgang Skorupa,[2] Bengt G. Svensson,[1] and Edouard Monakhov[1]
[1]*Department of Physics/Centre for Materials Science and Nanotechnology, University of Oslo, P. O. Box 1048 Blindern, N-0316 Oslo, Norway*
[2]*Institute of Ion Beam Physics and Materials Research, Helmholtz-Zentrum Dresden-Rossendorf, P. O. Box 510119, 01314 Dresden, Germany*

(Received 8 May 2015; accepted 30 June 2015; published online 13 July 2015)

Shallow, Boron (B)-doped p^+ emitters have been realized using spin-on deposition and Flash Lamp Annealing (FLA) to diffuse B into monocrystalline float zone Silicon (Si). The emitters extend between 50 and 140 nm in depth below the surface, have peak concentrations between $9 \times 10^{19}\,cm^{-3}$ and $3 \times 10^{20}\,cm^{-3}$, and exhibit sheet resistances between 70 and 3000 Ω/□. An exceptionally large increase in B diffusion occurs for FLA energy densities exceeding $\sim 93\,J/cm^2$ irrespective of 10 or 20 ms pulse duration. The effect is attributed to enhanced diffusion of B caused by Si interstitial injection following a thermally activated reaction between the spin-on diffusant film and the silicon wafer. © *2015 AIP Publishing LLC*.
[http://dx.doi.org/10.1063/1.4926661]

Formation of p-type emitters in n-type crystalline Silicon (c-Si) solar cells is possible by several different schemes, e.g., implantation,[1,2] diffusion from a gas source,[3,4] and diffusion from a surface source.[5,6] All these schemes require high temperature treatments to drive in and electrically activate the dopants[1,3,5] to reduce the series resistance of the cell. However, if the duration of the treatments is long, the diffusion length will be significant, and a highly doped emitter may extend several μm into the c-Si. This reduces the blue response of the cell since high energy photons are absorbed close to the surface followed by a fast recombination of the generated electron-hole pairs.

Flash Lamp Annealing (FLA) is a technique in which Si can be heated to temperatures above its melting point within a few milliseconds.[7–9] Thus, FLA enables both a reduction in the thermal budget of solar cell processing and improvement of the blue response. FLA has already been shown to be suitable for annealing of implantation-induced damage[9,10] and for activation of implanted dopants.[11] Recently, FLA was also proved to be effective in forming shallow Phosphorous (P) emitters in Si by diffusion from a spin-coated P surface source.[12] In the case of solar cells, this also requires the implementation of alternative schemes of contacting, e.g., electroplating and use of advanced silver pastes,[13,14] since the ordinary screen printing technique can provoke shunting of shallow emitters.

In this study, it is demonstrated that shallow Boron (B) emitters can be formed in c-Si by spin coating and subsequent in-diffusion using FLA.

A 300 μm Float Zone (FZ) c-Si wafer (n-type with resistivity of $\rho \approx 2000\ \Omega$ cm) was rinsed using a standard RCA clean leaving the wafer surface hydrophilic and ensuring good adhesion of the spin-on diffusant (SOD). 2 ml of a polyboron SOD (Filmtronics B155 SOD) was then applied to the substrate and spun at 6000 rpm for 30 s yielding a ∼190 nm thick film with a B concentration of $\sim 9 \times 10^{21}\,cm^{-3}$, as determined by Rutherford Backscattering Spectrometry (RBS). The deposited film was then baked at 200 °C for 20 min and subsequently laser cut into samples of $2 \times 2\,cm^2$ in size before FLA processing.

Four capacitors with capability to be charged up to a voltage of 4.4 kV were discharged within 10 or 20 ms into a bank of Xenon lamps positioned above the sample.[15] This produces a short light flash which emits in a wavelength range where Si absorbs strongly, and the Si sample can be heated to temperatures well above its melting temperature within a few milliseconds. The annealing was undertaken in N_2-atmosphere and the relevant FLA processing parameters for the different samples are summarized in Table I. An energy density above $\sim 120\,J/cm^2$ leads to sample melting, signifying that $\sim 120\,J/cm^2$ corresponds to approximately 1414 °C.

After FLA, and prior to characterization, the SOD film was removed by chemical etching. The SOD film was very stable after FLA and could not be etched by HF alone.

TABLE I. FLA parameters and characteristics of the processed samples. The emitter depth is defined as where the B concentration drops below $1 \times 10^{17}\,cm^{-3}$.

Sample #	Pulse duration (ms)	Capacitor voltage (kV)	Energy density (J/cm^2)	Boron peak concentration (cm^{-3})	Emitter depth (nm)
1	10	3.3	83	9×10^{19}	50
2	10	3.4	88	2×10^{20}	70
3	10	3.5	93	2×10^{20}	80
4	10	3.6	100	3×10^{20}	140
5	10	3.7	105	2×10^{20}	120
6	20	3.3	83	2×10^{20}	60
7	20	3.4	88	2×10^{20}	65
8	20	3.5	93	3×10^{20}	130
9	20	3.6	100	2×10^{20}	140
10	20	3.7	105	2×10^{20}	125
11	20	4.4	147	1×10^{20}	>30 000

a)Electronic mail: h.n.riise@fys.uio.no

Hence, the film was oxidized in HNO_3:H_2SO_4 (1:1) before the HF treatment. The procedure was repeated several times (10–20) before the sample surface became hydrophobic after the final HF treatment indicating complete removal of the SOD film.

Secondary Ion Mass Spectrometry (SIMS) measurements to detect ^{11}B-ions were performed using a Cameca IMS 7f microanalyzer with 10 keV O_2^+-ions as the primary beam. The depth of the sputtered crater was measured by a Dektak 8 stylus profilometer and used to convert sputtering time to depth (assuming a uniform and time-independent erosion rate). A B-implanted reference sample was used to translate the measured ^{11}B signal to B concentration. The sheet resistance of the samples was measured at room temperature by a four point probe Jandel KM3-AR setup. Transmission Electron Microscopy (TEM) analysis was performed on sample # 8 using an image-corrected FEI Titan 80–300 microscope.

Fig. 1 presents B profiles of all samples in a logarithmic depth scale with the melting of sample # 11 giving rise to an extension of the B profile to more than 30 μm. The inset displays B profiles from samples produced by spin-on deposition and Rapid Thermal Annealing (RTA) for 40 s. In the samples subjected to high FLA densities, a B concentration above the solubility limit appears in the vicinity of the surface. However, the SIMS data from the first 10 nm have limited validity since steady-state conditions for the measurements are not fully established and no definite conclusion on the possible existence of Si-B precipitates can be made. For the samples flashed for 10 ms (# 1–5, filled symbols), sample # 1 has a low integrated B concentration in terms of emitter requirements, whilst samples # 2–5 show more suitable profiles with emitter depths between 70 and 140 nm (cf. Table I). For these depths, the photon wavelength penetrating the emitter is above 420 nm, and most of the available sunlight will be absorbed in the base; this estimate is based on the absorption coefficient values given by Green.[16] The peak concentrations are between 9×10^{19} cm^{-3} and 3×10^{20} cm^{-3} which exceeds the solid solubility limit of B in Si (2×10^{20} cm^{-3} at 1100 °C (Ref. 17)).

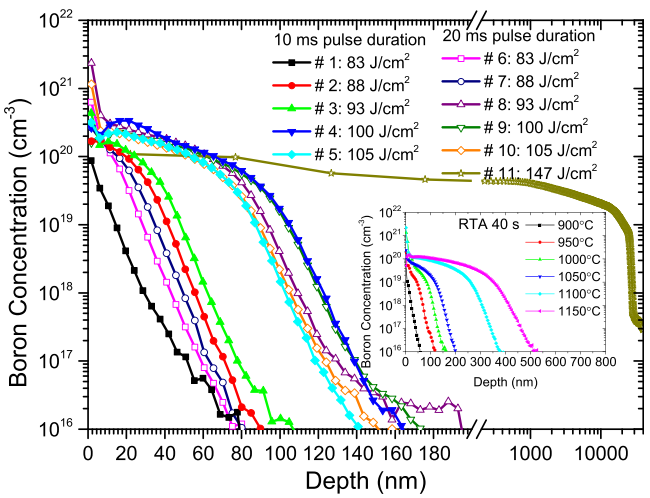

FIG. 1. Concentration of B as a function of depth for all samples. The inset displays data of samples treated by RTA for 40 s.

A similar conclusion can also be made from the data of the samples exposed to 20 ms FLA pulses (# 6–10, open symbols). The 20 ms profiles in Fig. 1 have an emitter depth between 60 and 140 nm with a peak concentration ranging from 2×10^{20} cm^{-3} to 3×10^{20} cm^{-3}, values similar to those of samples # 2–5.

Fig. 1 reveals two distinct sets of profiles; at energy densities below 93 J/cm^2 (10 ms duration) and 88 J/cm^2 (20 ms), a gradual increase in the peak concentration and emitter depth occurs (see, e.g., Table I). However, a further modest increase in the energy density leads to a considerable increase in both extension and peak concentration of the profiles with the emergence of a relatively flat, high B concentration plateau region. An increase above 93 J/cm^2 (20 ms) and 100 J/cm^2 (10 ms) does not significantly increase neither the emitter depth nor the peak concentration even though the resulting temperature increases by approximately 150 °C, in accordance with previous calibration.[15,18] In fact, the profile extension decreases (~20 nm) at 105 J/cm^2 relative to 100 J/cm^2, Fig. 1. Examining Fig. 1, it is also evident that the extension, peak concentration, and integrated B concentration of the deep profiles (# 4–5 and # 8–10) are almost independent of the pulse duration.

The corresponding sheet resistance values reveal high electrical activation of the incorporated B atoms as shown in Fig. 2. The filled, black squares and the filled, red circles represent the experimental sheet resistance values for samples # 1–5 and samples # 6–10, respectively. The calculated values (open symbols) were obtained by using the experimental SIMS-profiles (accounting for the isotopic abundance of ^{11}B) and Klaassen's mobility model[19] assuming full activation of all the incorporated B dopants. The samples # 2–5 and # 8–10 display values in the range of 70–260 Ω/□, which is appropriate for high efficiency solar cells. The calculated data follow the experimental values and point to a high activation ratio of B, although with some deviations presumably caused by inaccuracy of the mobility model.

The shape of the profiles of samples # 4–5 and # 8–10 in Fig. 1 resembles that in low energy B-implanted Si wafers subjected to Excimer Laser Annealing (ELA) and melting of the surface region.[20,21] The peak temperatures employed in our work are, however, well below that required for melting of Si (except for sample # 11, cf. Fig. 1). In fact, spin-on deposition and RTA for 40 s at 1050 °C and 1100 °C give rise to a similar abrupt increase in the profile extension as FLA at 93 J/cm^2 (20 ms) and 100 J/cm^2 (10 ms) (cf. the inset of Fig. 1), which indicates a threshold temperature between 1050 °C and 1100 °C for this abrupt increase. Partial melting of the samples as a cause of the increase in profile extension is hence ruled out. Further, it can be noted that RTA produces deeper profiles than FLA since the duration is much longer, and ordinary diffusion plays a larger role.

At the annealing temperatures and pulse durations used in this work, the equilibrium diffusion length of B in c-Si is only between 10 and 14 Å,[22] i.e., one to two orders of magnitude smaller than those in Fig. 1, clearly indicating nonequilibrium diffusion conditions reminiscent of so-called Transient Enhanced Diffusion (TED).[23] This is in direct contrast to that found in Ref. 12 for diffusion of P during FLA where no TED was observed nor any shrinkage of the profile

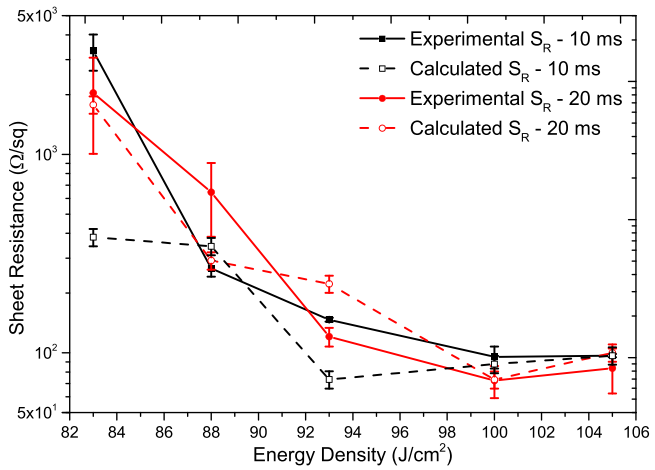

FIG. 2. Sheet resistance of all samples with calculated data deduced from the SIMS profiles using Klaassen's mobility model.[19] The calculations account for the natural abundance of ^{10}B and ^{11}B.

depth after high density FLA. Further, the temperatures used in Ref. 12 for similar extensions of the P profiles as those of the B profiles in Fig. 1 were about 200–300 °C higher. B diffusion in Si is primarily governed by an interstitialcy mechanism,[24] $B_S + I \rightleftharpoons BI$, where B_S represents the immobile (substitutional) configuration, I is the Si self-interstitial, and BI is the mobile (interstitial) configuration of B. Hence, an excess concentration of I's leads to enhanced diffusion of B and can account for the nonequilibrium diffusion seen in Fig. 1. Further, an I can also recombine with a Si vacancy, V, through the reaction, $I + V \rightarrow \varnothing$, i.e., V and B_S compete as traps for I.

The SSuprem4 process simulator, within Silvaco's Athena framework,[25] has been employed to simulate B-diffusion profiles assuming an excess of I's at the Si surface. A c-Si surface layer with a thickness of 190 nm, B-concentration of $9 \times 10^{21}\,\mathrm{cm}^{-3}$, and a certain concentration of excess I's was assumed as the diffusion source in the simulations. Fig. 3(a) shows simulated profiles for a 10 ms FLA pulse with peak $T = 1060\,^{\circ}\mathrm{C}$ using different excess initial I concentrations in the source, $C_{I,s}$. The FLA pulse is simulated to emulate the shape of the experimental FLA pulse given in Ref. 26. A drastic increase in the emitter depth is seen by comparing results without excess I's (black squares) and with excess I's (colored symbols), corroborating that the big leap in the experimental profiles for FLA densities at 93 J/cm^2 (20 ms) and 100 J/cm^2 (10 ms), Fig. 1, is governed by a sudden (transient) excess of I's at the surface. Also shown in Fig. 3(a) is a comparison between 5, 10, 20, and 60 ms pulses while keeping $C_{I,s}$ constant at $2 \times 10^{18}\,\mathrm{cm}^{-3}$ and $T_{peak} = 1060\,^{\circ}\mathrm{C}$. The resulting profiles overlap closely, which is consistent with the SIMS data in Fig. 1 for the samples flash lamp annealed with energy densities of 100 J/cm^2 and 105 J/cm^2, and pulse durations of 10 and 20 ms. This evidences that the temperature evolution in the samples is dominated by the heat dissipation after the flash rather than by the heating phase of the FLA treatment; the former has a characteristic rate of 400 °C/s, while the latter is much faster with a rate of 50–100 °C/ms.[18]

The decrease in emitter width for the highest (non-melting) FLA density used (105 J/cm^2) is surprising, see Fig. 1 and Table I, and it suggests that the B diffusion is retarded at high temperatures. Indeed, this suggestion is supported by the simulation results in Fig. 3(b) showing how the profile width gradually shrinks when the temperature exceeds 1080 °C (10 ms pulse and $C_{I,s} = 2 \times 10^{18}\,\mathrm{cm}^{-3}$). The shrinkage arises from a lower concentration of excess I's available to mediate the B diffusion at high temperatures because of a strongly increasing concentration of V's (Fig. 3(c)) leading to a higher recombination rate of the I's ($I + V \rightarrow \varnothing$). In other words, at high temperature, the V's becomes a serious competitor to B's for trapping of the highly mobile I's and less B is transformed into the mobile BI configuration. Here, it should be underlined that the formation energy of self-interstitials is substantially higher than that of the vacancies

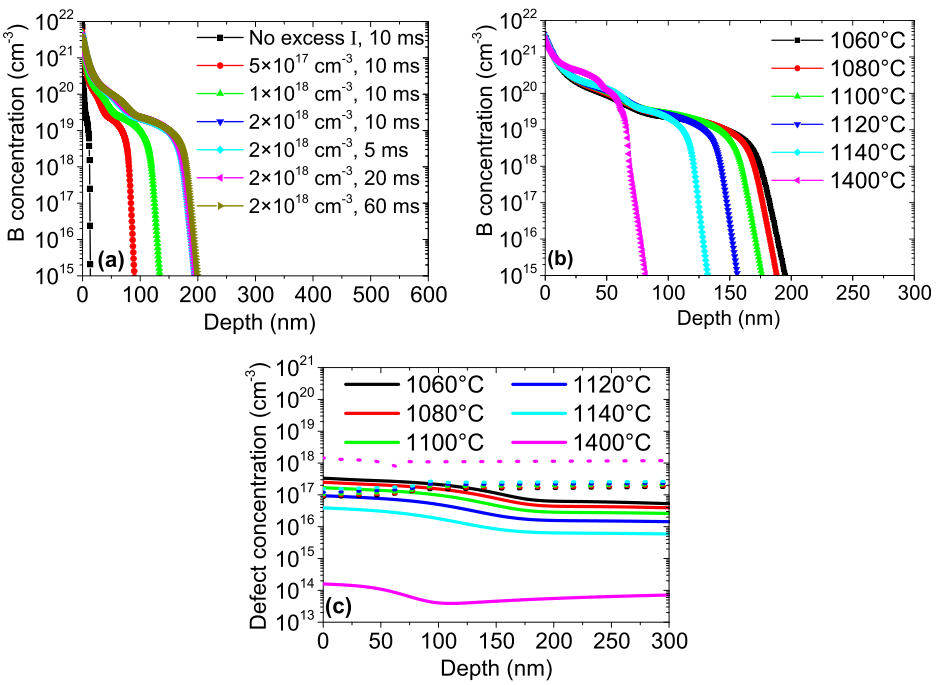

FIG. 3. Simulated boron and defect concentrations as a function of depth. (a) B profiles. Constant $T = 1060\,^{\circ}\mathrm{C}$ with varying $C_{I,s}$. (b) B profiles. Constant $C_{I,s} = 2 \times 10^{18}\,\mathrm{cm}^{-3}$ and $t = 10$ ms with varying T. (c) I (solid lines) and V (dotted lines) profiles. Constant $C_{I,s} = 2 \times 10^{18}\,\mathrm{cm}^{-3}$ and $t = 10$ ms with varying T.

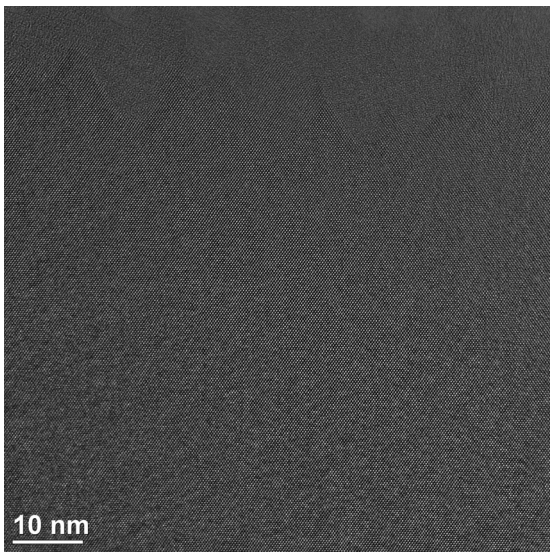

FIG. 4. High resolution TEM micrograph of the surface region of sample # 8. No crystal defects are observed.

(2.36 versus 1.08 eV)[25] and the equilibrium concentration of I's remains negligible to the excess one even at temperatures approaching the melting point.

As discussed above, a temperature above ~1050 °C is required for the enhanced B diffusion to occur; the process is thus thermally activated and provides evidence of TED. Data from RBS analysis give a composition of ~25% B, 55% C, and 20% O of the SOD film. Accordingly, at least two possible mechanisms can be put forward for injection of excess I's: (i) for a B-to-Si ratio above ~0.01 at the SOD/Si interface and temperatures below ~1270 °C, a mixture of Si, SiB_3, and SiB_6 co-exists at the Si surface.[27,28] The formation of such silicon boride precipitates, which is likely under the FLA conditions used, is accompanied by a large amount of released/injected I's. (ii) Because of the high oxygen content in the SOD films, formation of SiO_2 is anticipated at SOD/Si interface leading to injection of I's, i.e., so-called oxidation-enhanced-diffusion (OED).[29] Further investigations need to be pursued in order to unveil the relative importance of these two processes.

In Fig. 4, a TEM image of the surface region of sample # 8 is shown. Neither the surface region nor the junction region (not included) exhibits structural defects, demonstrating that the FLA treatment does not induce a high defect concentration. The roughness (≲10 nm) observed at the top of the image is due to the post-FLA etching treatment and may partially limit the SIMS depth-profiling resolution (~10 nm). Further, no secondary phases (such as SiB_3 or SiB_6) are observed in the bulk of Si (deeper than 5–10 nm). The lack of TEM evidence for precipitates does, however, not preclude their presence *during* FLA as the precipitates may have been etched away by the chemical treatment prior to TEM characterization.

In conclusion, by depositing a polyboron SOD on a Si wafer and heat treating the system with FLA for 10 or 20 ms, high concentration shallow p^+ emitters have been realized. The emitters are highly electrically activated with B peak concentrations between $9 \times 10^{19}\,cm^{-3}$ and $3 \times 10^{20}\,cm^{-3}$ and depths between 50 and 140 nm. TEM analysis reveals no structural defects induced by the FLA treatment. A drastic broadening of the B profiles occurs above an energy density of 88 J/cm^2, attributed to TED mediated by Si self-interstitials as supported by process simulations. The interstitials originate most likely from a thermally activated reaction between the SOD film and the Si wafer surface.

This work was performed within "The Norwegian Research Centre for Solar Cell Technology" (Project No. 460976), a Centre for Environment-friendly Energy Research cosponsored by the Norwegian Research Council and research and industry partners in Norway.

[1]B. J. Pawlak, T. Janssens, S. Singh, I. Kuzma-Filipek, J. Robbelein, N. E. Posthuma, J. Poortmans, F. Cristiano, and E. M. Bazizi, Prog. Photovoltaics **20**, 106 (2011).
[2]N. Bateman, P. Sullivan, C. Reichel, J. Benick, and M. Hermle, Energy Procedia **8**, 509–514 (2011).
[3]Y. Komatsu, V. Mihailetchi, L. Geerligs, B. van Dijk, J. Rem, and M. Harris, Sol. Energy Mater. Sol. Cells **93**, 750 (2009).
[4]M. A. Kessler, T. Ohrdes, B. Wolpensinger, and N. P. Harder, Semicond. Sci. Technol. **25**, 055001 (2010).
[5]F. Recart, I. Freire, L. Perez, R. Lago-Aurrekoetxea, J. Jimeno, and G. Bueno, Sol. Energy Mater. Sol. Cells **91**, 897 (2007).
[6]R. R. King and R. M. Swanson, IEEE Trans. Electron Devices **38**, 1399 (1991).
[7]H. A. Bomke, H. L. Berkowitz, M. Harmatz, S. Kronenberg, and R. Lux, Appl. Phys. Lett. **33**, 955 (1978).
[8]R. L. Cohen, J. S. Williams, L. C. Feldman, and K. W. West, Appl. Phys. Lett. **33**, 751 (1978).
[9]J. T. Lue, Appl. Phys. Lett. **36**, 73 (1980).
[10]R. Klabes, J. Matthxi, M. Voelskow, G. A. Kachurin, E. V. Nidaev, and H. Bartsch, Phys. Status Solidi A **66**, 261 (1981).
[11]T. Ito, T. Iinuma, A. Murakoshi, H. Akutsu, K. Suguro, T. Arikado, K. Okumura, M. Yoshioka, T. Owada, Y. Imaoka, H. Murayama, and T. Kusuda, Jpn. J. Appl. Phys., Part 1 **41**, 2394 (2002).
[12]H. B. Normann, L. Vines, V. Privitera, W. Skorupa, T. Schumann, B. G. Svensson, and E. V. Monakhov, Appl. Phys. Lett. **102**, 132108 (2013).
[13]S. W. Glunz, Adv. OptoElectron. **2007**, 97370 (2007).
[14]Z. G. Li, L. Liang, A. S. Ionkin, B. M. Fish, M. E. Lewittes, L. K. Cheng, and K. R. Mikeska, J. Appl. Phys. **110**, 074304 (2011).
[15]T. Gebel, M. Voelskow, W. Skorupa, G. Mannino, V. Privitera, F. Priolo, E. Napolitani, and A. Carnera, Nucl. Instrum. Methods Phys. Res., Sect. B **186**, 287 (2002).
[16]M. A. Green, Sol. Energy Mater. Sol. Cells **92**, 1305 (2008).
[17]C. Zaring, A. Pisch, J. Cardenas, P. Gas, and B. G. Svensson, J. Appl. Phys. **80**, 2742 (1996).
[18]T. Schumann, private communication (2015).
[19]D. B. M. Klaassen, Solid-State Electron. **35**, 953 (1992).
[20]P. Baeri, S. U. Campisano, G. Foti, and E. Rimini, J. Appl. Phys. **50**, 788 (1979).
[21]E. V. Monakhov, B. G. Svensson, M. K. Linnarsson, A. L. Magna, C. Spinella, C. Bongiorno, V. Privitera, G. Fortunato, and L. Mariucci, Appl. Phys. Lett. **86**, 151902 (2005).
[22]P. M. Fahey, P. B. Griffin, and J. D. Plummer, Rev. Mod. Phys. **61**, 289 (1989).
[23]P. A. Stolk, H.-J. Gossmann, D. J. Eaglesham, D. C. Jacobson, C. S. Rafferty, G. H. Gilmer, M. Jaraiz, J. M. Poate, H. S. Luftman, and T. E. Haynes, J. Appl. Phys. **81**, 6031 (1997).
[24]W. Windl, M. M. Bunea, R. Stumpf, S. T. Dunham, and M. P. Masquelier, Phys. Rev. Lett. **83**, 4345 (1999).
[25]*Athena User's Manual, Silvaco, Inc.*, 2014.
[26]W. Skorupa, T. Gebel, R. A. Yankov, S. Paul, W. Lerch, D. F. Downey, and E. A. Arevalo, J. Electrochem. Soc. **152**, G436 (2005).
[27]R. W. Olesinski and G. J. Abbaschian, Bull. Alloy Phase Diagrams **5**, 478 (1984).
[28]T. L. Aselage, J. Mater. Res. **13**, 1786 (1998).
[29]S. M. Hu, J. Appl. Phys. **45**, 1567 (1974).